Desalination and Water Treatment
www.deswater.com
doi: 10.1080/19443994.2013.855671

53 (2015) 1591–1605
February

Taylor & Francis
Taylor & Francis Group

Iron-impregnated activated carbons precursor to rice hulls and *areca* nut waste in the remediation of Cu(II) and Pb(II) contaminated waters: a physico-chemical studies

Diwakar Tiwari[a], Lalhmunsiama[a,b], Seung-Mok Lee[b,*]

[a]*Department of Chemistry, School of Physical Sciences, Mizoram University, Aizawl 796004, India*
[b]*Department of Environmental Engineering, Kwandong University, Gangnung, Gangwondo 210701, Korea*
Tel. +82 33 649 7535; Fax: +82 33 642 7635; email: leesm@kwandong.ac.kr

Received 23 May 2013; Accepted 3 October 2013

ABSTRACT

The aim of this study is to exploit the abundantly available rice hulls and *areca* nut waste in obtaining the activated carbons which is further impregnated with a low dose of iron to obtain the iron-impregnated activated carbon (IIAC) samples. The solids are characterized by the IR and XRD analytical tools whereas the surface morphology is discussed with the SEM images of these solids. BET specific surface area which was obtained for these materials showed that the impregnation of iron did not significantly affect the specific surface area of these solids. Further, the materials were employed in the removal of two different heavy metal toxic ions *viz*. Cu(II) and Pb(II) under the batch and column reactor operations. The batch data were collected for various physico-chemical parametric studies, *viz*. effect of solution pH, sorptive concentration, contact time, electrolyte concentrations, etc. The mechanism involved at solid/solution interface was discussed with the help of these studies. Moreover, the equilibrium state sorption data and the time dependence data were utilized to conduct the adsorption isotherm and kinetic modeling studies, respectively. The pseudo-second-rate equation was fitted well to the sorption of these two cations; hence, the sorption capacity was estimated to be 1.770 and 1.926 mg/g (for Cu(II)) and 3.507 and 3.439 mg/g (for Pb(II)), respectively for IIAC-R and IIAC-N. The removal of these two cations was also performed under the dynamic experimentations under column studies. The column data were utilized obtaining the breakthrough curves and hence the breakthrough volumes were obtained. Further, the breakthrough data were utilized to simulate it with Thomas equation and, hence, the loading capacity of the columns was estimated to be 2.746 and 3.057 mg/g (for Cu(II)) and 6.957 and 6.505 mg/g (for Pb(II)), respectively for IIAC-R and IIAC-N samples.

Keywords: Iron-impregnated activated carbons; Porous materials; Sorption; Kinetics; Breakthrough curve

1. Introduction

Heavy metal contamination of aquatic environment is one of the serious global problems. These heavy metals neither can be degraded to harmless end products nor can be easily removed from the aquatic environment with usual treatment processes. Moreover, they accumulate within the biosystem and cause several biological disorders. Although copper is

*Corresponding author.

known to be an essential metal ion required for several metabolic functions at a low level, higher concentration poses serious threat to its varied toxic effects [1]. The common toxic effects reported are irritation of the nose, mouth, and eye, leading to headache, stomachache, dizziness, vomiting, and diarrhea. Liver and kidney damage possibly occurs with much enhanced intake of copper. On the other hand, lead is one of the non-essential toxic ions, which possesses several toxic and environmental issues even at a very low level. It may interfere with several metabolic processes of several organs and tissues including heart, bones, intestine, kidney, reproductive system, nervous system or even the damage of brain [2]. The USEPA suggested the limit for copper and lead presence in the drinking water as 1.3 ppm and 15 ppb, respectively. Therefore, the aquatic environment contaminated with these heavy metals needs a special treatment method for its removal from aqueous solutions as to meet the stringent regulatory laws laid down by the regulatory authority.

The role of activated carbon (AC) in the advanced treatment of wastewater or industrial wastewater has received a greater attention in the last few decades because of its porous structures—micro-and meso-pores; surface functional groups—Bronsted acid/base property; and relatively high specific surface area [3–7]. Commercially available ACs were obtained from different carbonaceous bulk materials and their physical and chemical properties were reported to be varied with the precursor materials as well as with the method of activation. Moreover, the commercial products are found to be costly for the bulk treatment of the waste/industrial waters. However, the use of natural agricultural by-products or waste dead biomasses has gained momentum in recent past as alternative precursor materials for obtaining ACs. This could perhaps provide cheaper and effective treatment processes and also alleviate the problem of waste disposal [1,8]. In a line, several natural agricultural waste materials were employed to obtain the ACs and employed in the treatment of heavy metal toxic ions along with the variety of dyes, antibiotics etc. from aquatic environment [9–19]. A film-pore diffusion model was utilized in the removal of lead, copper, chromium, and cobalt under the batch and fixed bed operations using the granular ACs [20]. Similarly, the ACs were found to be a suitable filter medium; the selectivity and suitability of the AC were enhanced for several heavy metal toxic ions by impregnating it with iron or manganese [21–24]. Moreover, the iron impregnation in AC makes an additional advantage of easy magnetic separation from the bulk solution using a simple magnet. It was further reported that iron-modified activated carbon derived from Golbasi lignite showed significantly a higher adsorptive removal capacity for cyanide than its precursor AC [25]. Multi-wall carbon nanotube (CNT) was modified with iron oxide so as to magnetize the sorbent in the removal of Cr(III) from the aquatic environment [26]. Similarly, MnO_2/CNT nanocomposite was utilized in the fixed bed column studies for the removal of Pb(II) from aqueous solutions [27].

The present study attempted to obtain the AC samples precursor to the rice hulls and *areca* nut waste. The high specific surface area with porous structure was further utilized to impregnate the iron-oxide particles onto the AC so as to obtain suitable and selective iron-impregnated activated carbon (IIAC) materials. These materials were further employed in the decontamination of an aquatic environment contaminated with two important heavy metal toxic ions, *viz.* copper(II) and lead(II), under the batch and fixed bed column operations.

2. Materials and methods

2.1. Materials

The dead biomasses *viz.* rice hulls and the *areca* nut wastes were collected from Aizawl, Mizoram, India. Sulphuric acid and ammonia were obtained from the Merck, India. The manganese nitrate as Mn $(NO_3)_2.6H_2O$ which was 97% extra pure and lead nitrate were obtained from the Junsei Chemical Co. Ltd., Japan, and iron(III) nitrate enneahydrate was obtained from the Kanto Chemicals Co. Inc., Japan. The copper sulphate, sodium hydroxide and nitric acid were obtained from the Duksan Pure Chemicals Co. Ltd., Korea. The deionized water was purified further by the Millipore water purification system (Milli-Q^+).

2.2. Preparation of AC

The raw biomass materials i.e. rice husk and *areca* nut wastes were collected locally and washed with the deionized distilled water. Samples were dried at 60˚C in a drying oven. Dried biomasses (each 150 g) were digested in a concentration of H_2SO_4 (50 mL) and the content was kept at 120˚C for 2 h. The carbonized carbon obtained was washed with the distilled water as to obtain the filtrate pH~4.0. Again, the samples were dried at 70˚C and then titrated with a small volume of NH_3 solution (10 mL; 36%) to neutralize the excess acid. The solid sample was washed with the distilled water and

completely dried at 70˚C. It was cooled at room temperature and ground to fine powder. Further, this carbonized carbon was activated by using a muffle furnace at 800˚C in an N_2 environment for 3 h and the ACs obtained from the rice husk and *areca* nut waste were termed as AC-R and AC-N, respectively. These solids were further employed in the preparation of iron-oxide-impregnated activated carbons (*viz*. IIAC-R and IIAC-N).

2.3. Preparation of iron oxide impregnated activated carbons

To prepare iron-oxide-impregnated activated carbons (IIACs), 60 g of AC was taken in a round-bottom flask with 100 mL of 0.025 M iron nitrate solution (pH~9) and was kept in a rotary evaporator at 60˚C at the rotating speed of 30 rpm. Further, from *Ca*, 90% of the water was removed by applying slowly the vacuum. The slurry was taken out in a beaker and kept in a drying oven at 90˚C to dry the solids completely. It was further kept at 110˚C for 2 h for the stabilization of immobilized iron-oxide particles onto the solid surface. Samples were taken out from the drying oven and cooled at room temperature and washed again with the distilled water. It was dried at 70˚C and stored in airtight polyethylene bottles.

2.4. Characterization of the materials

The solids obtained were characterized by the IR (Bruker, Tensor 27, USA by KBR disk method) and XRD (X-ray diffraction machine i.e. PANalytical, Netherland; Model X'Pert PRO MPD) methods. The XRD data were collected with the scan rate of 0.034 of 2θ illumination at an applied voltage of 45 kV with an observed current of 35 mA, using CuK_α radiations having a wavelength of 1.5418 Å. The surface morphology of these solids was obtained by the SEM/EDX (scanning electron microscope model: FE-SEM-Model: SU-70, Hitachi, Japan; equipped with an energy dispersive X-ray spectroscopy EDX system) analysis. The BET specific surface area was obtained by the Protech Korea BET surface area analyzer (Model ASAP 2020). Further, the amount of iron content in IIACs was determined by the standard US EPA (3050B) method. Moreover, the stability of the impregnated manganese and iron oxides was ascertained at a wide range of pH i.e. pH from 2.0 to 10.0 and it was revealed that the coating was fairly stable within the pH region from 3.0 to 10.0 since an insignificant amount of the iron was leached into the bulk solution.

2.5. pHpzc determination of the solids

The pHpzc (point of zero charge) of these solids (i.e. ACs and IIACs) was obtained by using the known method as described earlier [28,29]. Briefly, it was carried out as follows. First, 500 mL of double distilled water was taken in an Erlenmeyer flask capped with cotton. It was slowly but continuously heated until boiling for 20 min so as to expel the dissolved CO_2. The flask was capped immediately to prevent re-absorption of atmospheric CO_2 by water. Then, 50 mL of 0.01 M NaCl solutions was prepared using CO_2-free water and taken in two different bottles. The pH of each solution in each flask was adjusted to its pH values of 2.0, 4.0, 6.0, 8.0, 10.0 and 12.0 by adding 0.1 M HCl or 0.1 M NaOH, solutions. Then, 0.15 g of the solid sample was introduced in each bottle and agitated for 24 h at 25˚C, and the solutions were filtered and its final pH was measured using a pre-calibrated pH meter. The pHpzc was taken as the point at which the curve crossed the line where pH_{final} equals to $pH_{initial}$.

2.6. Batch reactor operations

Batch experiments were carried out to obtain the adsorption data with a variation in sorptive pH, contact time, initial metal concentration, and electrolyte concentrations. The stock solutions of 100 mg/L of Cu(II) and Pb(II) was prepared by dissolving an accurate amount of their respective salts in the distilled water and further diluted to its required experimental concentration by successive dilution process. The adsorption of Cu(II) or Pb(II) was investigated by taking 0.25 g of IIACs solids separately in 100.0 mL of sorptive solution having known the concentration of Cu(II) or Pb(II). The solution mixture was equilibrated by using an automatic shaker (KUKJE, Shaking Incubator, Korea model 36-SIN-125) for 24 h at 25˚C temperature. The solution was then filtered with a 0.45 μm syringe filter, and the final pH was measured and reported. The filtered solutions were subjected for AAS analysis (Fast Sequential Atomic Absorption Spectrometer: Model AA240FS, Varian) to obtain the final metal concentrations. The percent removal was calculated as stated elsewhere [30]. Adjustment of the pH was done by the dropwise addition of HNO_3 or NaOH concentration. The time dependence data were collected at different time intervals.

Similarly, the sorbate concentration dependence data were collected by taking the M(II) concentrations from 1.0 to 20.0 mg/L (25.0 mg/L for Cu(II)) at a onstant pH ~4.0 and at a constant temperature 25 ± 1˚C.

The sorption process was carried out as described before. Further, the equilibrium concentration dependence sorption data were employed in equilibrium modeling studies using the Freundlich and the Langmuir adsorption isotherms as discussed elsewhere [30,31].

The electrolyte concentration dependence study was carried out by varying the electrolyte concentration of sorptive solutions from 0.001 to 1.0 mol/L of $NaNO_3$ keeping the solution pH (~4.0) and temperature (25 ± 1°C) constant throughout. Results were presented as percent removal as a function of electrolyte concentrations.

2.7. Column studies

The column experiments were performed using a glass column (1 cm in inner diameter) packed with 1.0 g of IIACs (kept middle in the column); below and above to this, 1.0 g each of bare sand (30–60 BSS in size) was kept and then it was packed with glass beads. The sorbate solutions i.e. Cu(II) or Pb(II) (10.0 mg/L) having pH 4.0 was pumped upward from the bottom of the column using a Acuflow Series II, high-pressure liquid chromatograph; at a constant flow rate of 1.00 mL/min. Effluent samples were then collected using a Spectra/Chrom CF-2 fraction collector. The collected samples were filtered with a 0.45 μm syringe filter and the total bulk sorbate concentration was measured using AAS.

3. Results and discussion

3.1. Characterization of materials

The ACs obtained from the rice hulls and *areca* nut waste along with the IIACs were analyzed with the FT-IR analytical tool and results were presented graphically in Fig. 1(a) and (b), respectively, for the rice hulls and *areca* nut. The carbon samples may possess various functional groups having different surface structures *viz*. aliphatic, aromatic, and cyclic since the IR bands were observed at around 1,480 and 1,110 cm^{-1}. Predominant and broad peaks appeared at around 3,470 cm^{-1} were ascribed to the stretching vibration of –OH groups (carboxyl, alcohol or phenols), etc. [1]. However, it was reported that the IR bands occurred at around 3,300 and 3,250 cm^{-1} were indicative of the hydroxyl groups. Further, the band was shifted at around 3,500 cm^{-1} in case of non-bonded alcohols, phenols, and carboxylic acids [32]. Vibration peaks occurred in between 2,930 and 2,910 cm^{-1} were ascribed to the C–H stretching and C–H scissoring bands. Moreover, it was suggested that the peaks at 2,800–2,900 cm^{-1} were indicated to the existence of aldehyde groups [1]. A weak peak occurred at around 1,460 cm^{-1} showed the C–H vibration in $–CH_2–$ deformation [33]. Moreover, the bands occurred in between 1,600 and 1,400 cm^{-1} (more predominant in the *areca* nut ACs) could be assigned as C=C vibrations. It was pointed that the peaks in the region 1,350–900 cm^{-1} was because of the C–O or C=O vibrations [34]. Similarly, a vibration band occurred around 870 cm^{-1} was obtained because of an external bending of –C–H for different substituted benzene rings [35]. A peak at around 450–470 cm^{-1} showed the presence of α-Fe_2O_3 [36] in both IIAC samples. Moreover, this peak, which was also present in both AC samples but with less intensity, indicated that the bare ACs also included with some iron oxide, which was again confirmed with the digestive analysis conducted separately. Similarly, the peaks at around 840 cm^{-1} inferred to the υ_s vibrations of Si–O–Si or δ–Fe–OH vibrations predominant in the rice hulls AC samples [37].

Further, the samples were subjected for the X-ray diffraction analysis and the results were presented graphically in Fig. 2. It was observed that the AC obtained by rice hulls possessed a diffraction peak at 2θ value of 22.5 which showed a characteristic

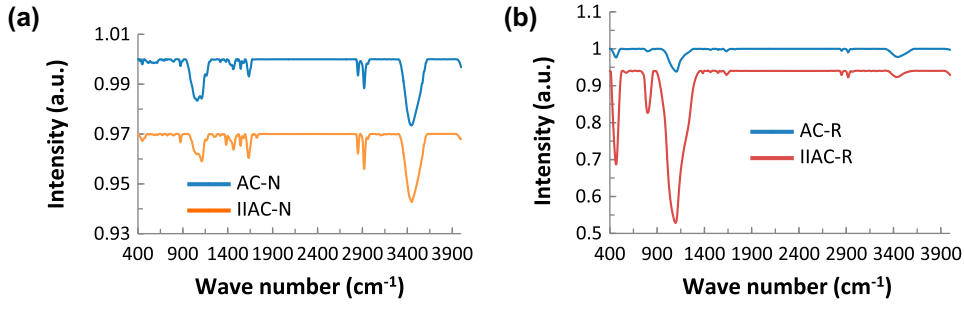

Fig. 1. FT-IR data obtained for the (a) AC-N and IIAC-N and (b) AC-R and IIAC-R solids.

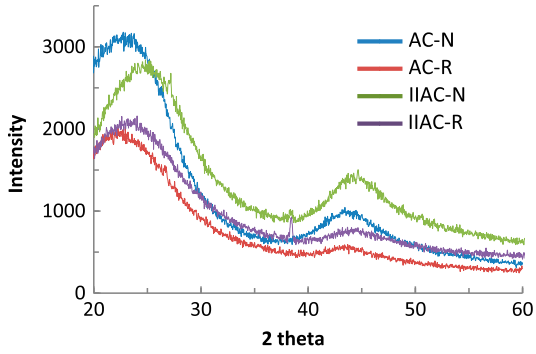

Fig. 2. XRD pattern obtained for the ACs and IIACs solids.

peak of amorphous silica [38]. Similarly, the AC of *areca* nut showed very broad diffraction peak almost in the same region indicating, perhaps, the amorphous, silica. The XRD data further indicated that ACs have no ordered crystalline structure since no sharp reflections were observed for these samples. Similar to corresponding AC samples, the IIAC-R and IIAC-N showed almost an identical XRD pattern except a weak but sharp peak at the 2θ value of 39, which is an indicative of *akaganeite* (β-FeOOH) mineral phase of iron [39]. Possibly, the other diffraction peak of the *akaganeite* at 2θ value of 35 was missing because of a low content of iron or of a weak diffraction at this 2θ value [25]. Previously, it was observed that the iron impregnated with the different substrates hardly showed sharp XRD diffractions, perhaps, because of the amorphous iron deposited or the particles were significantly small to diffract or even because of very low content of iron [5,25,40].

The surface was morphologically obtained by the SEM images of these solids and presented in Fig. 3. The SEM images clearly indicated that the surface morphology of iron-impregnated sample was changed significantly comparing to its precursor AC samples. Surface structure of AC showed very porous surface and the pores were very unevenly distributed on the surface. The pores on the AC-N surface were opened partly, however, mostly distributed evenly on the surface. The pore size varies significantly for these solids. Moreover, comparing AC-R, the AC-N possessed more porous surface structure. The silicon oxide available with the rice hulls was aggregated on the surface or within the pores of AC-R making the surface more heterogeneous. Further, the SEM images of IIACs showed that the iron-oxide (possibly α-Fe_2O_3 or β-FeOOH mineral phases) particles were significantly aggregated or even clustered onto the surface of AC samples or even within the pores of the ACs. The particles were distributed unevenly and predominantly small in size. The previous report indicated that the nano-sized manganese dioxide or iron-oxide particles were distributed orderly onto the sand surface providing a distinct specific surface area [41,42]. These results, therefore, indicated that the iron-oxide particles were significantly impregnated on to the surface of AC-N and AC-R.

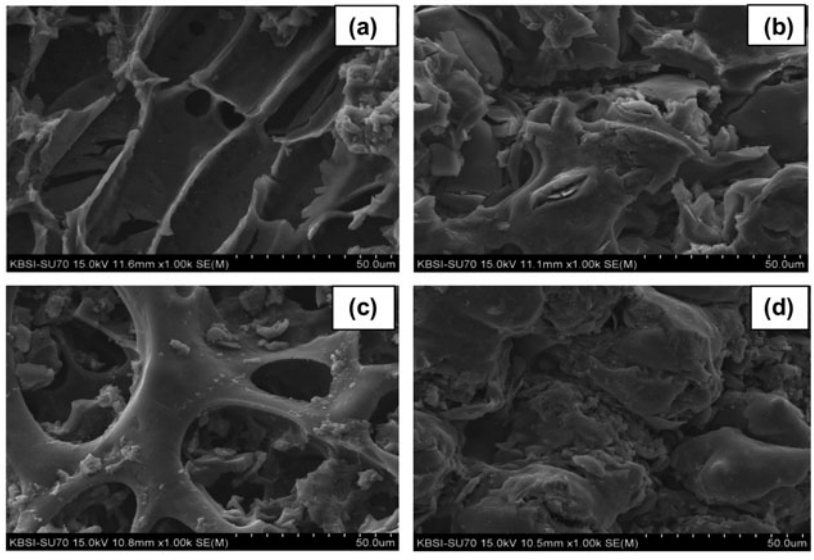

Fig. 3. SEM images of (a) AC-N, (b) AC-R, (c) IIAC-N, and (d) IIAC-R.

The BET specific multi-point surface area was obtained for these solids and found to be 379.77, 322.14, 370.88, and 303.79 m^2/g, respectively, for the AC-N, AC-R, IIAC-N, and IIAC-R solids. The significant specific surface area obtained for the AC samples was, therefore, employed for the impregnation of iron oxide onto these solids. The specific surface area of AC was slightly decreased in the presence of iron oxide since the iron occupied the spaces and hence decreased the specific surface area. The similar decrease in specific area was reported previously in the case of iron-doped activated carbon sample [24], whereas the iron- or manganese-impregnated sand showed an enhanced specific surface area compared to the bare sand because of the very compact structure of sand [42].

Further, the effective amount of iron content of the samples was analyzed by the US EPA 3050B acid digestion method. The iron content was found to be 107.0, 39.0, 2442.0, and 2221.0 mg/kg, respectively, for the solids AC-N, AC-R, IIAC-N, and IIAC-R. This clearly showed that these ACs contained some amount of iron content, which possibly resulted in the IR peaks as revealed previously. Moreover, IIACs possessed a significant amount of iron.

3.2. Batch reactor studies

3.2.1. Effect of pH

The pH dependence study was conducted for it could enable us to discuss the mechanistic aspects involved in the solid/solution interface. The pH dependence sorption data were represented graphically in Fig. 4(a) and (b), respectively, for the Cu(II) and Pb(II) removal. It was, in general, observed that increasing the pH from 2.0 to 10.0 apparently caused an increase in the percent removal of these two studied cations. More precisely, for the increase in the pH from 2.22 to 9.16 (for IIAC-R) and from 2.24 to 9.33 (for IIAC-N), the corresponding increase in the percent removal of Cu(II) was, respectively, from 4.57 to 100% and from 4.11 to 100%. Similarly, for the increase in pH from 2.04 to 9.99 (for IIAC-R) and 2.08 to 9.66 (for IIAC-N), the corresponding removal of Pb(II) was found to be, respectively, from 12.17 to 98.17% and 5.78 to 98.07%. Further, it was observed that a gradual but sharp increase in the uptake of Cu(II) or Pb(II) was occurred by these solids up to the pH around 6.0; after that, it slowed down. Interestingly, about 80% of the Cu(II) or Pb(II) was removed up until the pH was reached to 6.0. It showed that very high removal capacity was obtained at the neutral or slightly acidic pH region.

The mechanism of the adsorption process could be explained based on the surface properties of IIAC solids and the speciation of the Cu(II) and Pb(II) in solution within the studied pH range. The previous studies conducted for the Cu(II) and Pb(II) speciation using the MINEQL computer simulation program showed that up to pH 5.8 both Cu(II) and Pb(II) were present only as in the cationic forms i.e. Cu^{2+} and Pb^{2+} and carrying a net positive charge [41]. Beyond this, it started to convert into tenorite and $Pb(OH)_2$ solid forms, respectively, for Cu(II) and Pb(II) which attained almost 100% at around pH 7.0. Moreover, insignificant i.e. max. 2–4% of $Cu(OH)^+$ and $Pb(OH)^+$ species occurred at pH 5.8 (for Cu(II)) and pH 6.0 (for Pb(II)). Therefore, the sorption occurred below pH 6.0 is dominant because of the cationic species of Cu(II) and Pb(II). On the other hand, the solid surface showed the pH_{PZC} for the solids IIAC-N and IIAC-R was 6.2 and 6.1, respectively. The surface hydroxyl groups were dominantly involved with the acidic dissociation and show the Bronsted acid base behavior. The acidic dissociation of surface functional groups could be represented as Eq. (1):

$$\equiv \text{S-OH}_2^+ \leftrightarrow \underset{\text{pH}_{\text{PZC}}}{\equiv \text{S-OH}^0} \leftrightarrow \equiv \text{S-O}^- \quad (1)$$

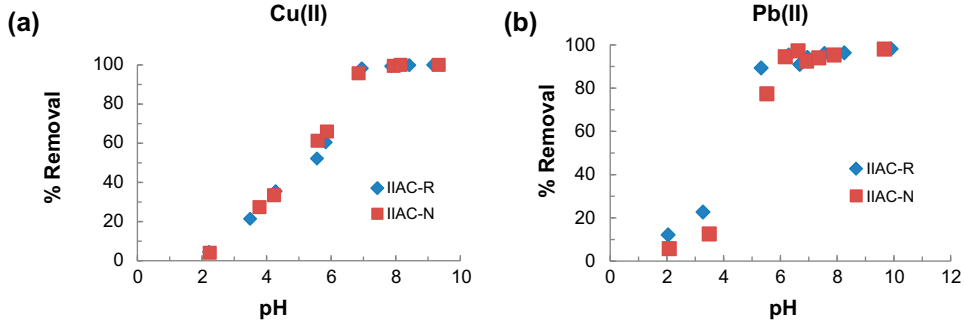

Fig. 4. Effect of solution pH in the percent sorption of (a) Cu(II), and (b) Pb(II) by using IIACs.

Significantly, low removal of Cu(II) or Pb(II) at low pH values i.e. pH around 2.0–4.0 could be ascribed because of strong electrostatic repulsive forces involved between the positively charged surface and metal cations [31,41]. Moreover, there could, perhaps, be a competition between the proton and cations for the same surface sites, which in turn decreased the percent removal of Cu(II) and Pb(II) from aqueous solutions [43,44]. The gradual increase in pH caused a gradual acidic dissociation of surface functional groups and enabled further the electrostatic attraction of metal cations towards the surface followed by a binding on the surface active sites. The surface binding of metal cations could be suggested as "inner sphere" monodentate and bidentate surface complexation:

$$\equiv \text{S-O}^- + \text{M}^{2+} \leftrightarrow \equiv \text{S-O-M}^+ \quad (2)$$

$$\equiv \text{S-O}^- + \text{M}^{2+} + \text{H}_2\text{O} \leftrightarrow \equiv \text{S-O-MOH} + \text{H}^+ \quad (3)$$

$$2 \equiv \text{S-O}^- + \text{M}^{2+} \leftrightarrow (\equiv \text{S-O})_2\text{M} \quad (4)$$

Eqs. (2) and (3) shows a monodentate binding and Eq. (4) shows a bidendate binding of metal cations. The similar reaction mechanism was proposed and modeled previously for the sorption of copper(II) onto the surface of AC [33]. It was observed that iron-coated or manganese-oxide-impregnated sand formed a similar Cu(II) and Pb(II) surface complexation via the ion exchange process [41,42].

Further, the increase in pH favored greatly the removal of these ions onto the solid surface. This could be because of the mixed effect of adsorption and co-precipitations since both these metal ions turned into insoluble precipitates beyond the pH~6.0 resulting in almost 100% of the removal. Moreover, a comparison of these two solids i.e. IIAC-R and IIAC-N showed an almost identical removal behavior throughout the entire pH-edge curves. This could be explicable with the fact that the driving force of the sorption was mainly due to the immobilized iron oxide; hence, the two solids possessed an identical sorption behavior separately for Cu(II) and Pb(II). Additionally, it was observed that the physical parameters *viz*. BET specific surface area and pH_{PZC} values of these two solids are also almost same for these two solids, which pointed it again for identical sorption behavior.

3.2.2. Effect of sorbate concentration

The concentration dependence data were collected varying the Cu(II) and Pb(II) concentration from 1.0 to 20.0 mg/L (25.0 mg/L for Cu(II)) at pH 4.0. Results obtained were given graphically in Fig. 5(a) and (b), respectively, for Cu(II) and Pb(II). It was observed that increasing the Cu(II) concentration from 1.45 to 25.60 mg/L caused a decrease in the percent removal of Cu(II) from 89.79 to 28.67% for IIAC-R and from 88.62 to 22.60% for IIAC-N. On the other hand, the very high percent removal of Pb(II) was almost unaffected with such an increase in concentration. This suggested the very high affinity of surface active sites for the Pb (II). The similar results were reported previously for the adsorption of Cu(II) and Pb(II) onto the sericite [31] or onto the granular AC obtained by the coconut shell [45].

3.2.3. Equilibrium state modeling

The equilibrium state sorption data were utilized to non-linear Langmuir and Freundlich adsorption isotherms as stated, respectively, in Eqs. (5) and (6):

$$q_e = \frac{q_m K_a C_e}{1 + K_a C_e} \quad (5)$$

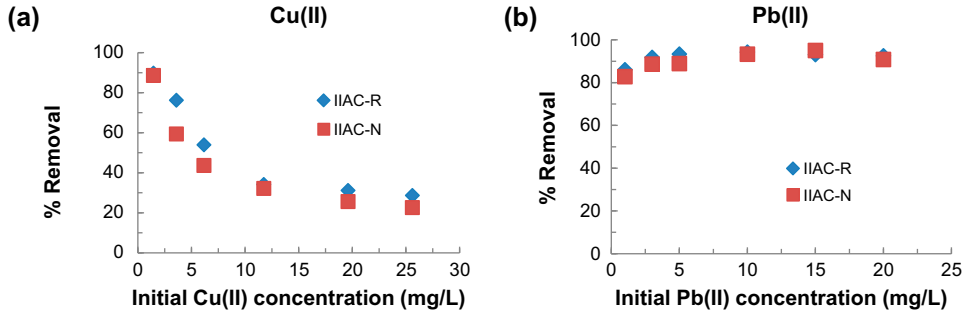

Fig. 5. Effect of sorptive concentration in the percent removal of (a) Cu(II) and (b) Pb(II) by using IIACs.

$$q_e = K_F C_e^{1/n} \quad (6)$$

where q_e and C_e are denoted the amount adsorbed and the bulk sorptive concentration at equilibrium, respectively. q_m and K_a are the Langmuir constants referred to the maximum monolayer capacity of solid and strength or affinity of solid towards the sorbing ions, respectively. Similarly, the K_F and $1/n$ are the Freundlich constants referred to the maximum sorption capacity and adsorption intensity, respectively.

The non-linear fitting of sorption data to above equations were performed and the results were presented graphically in Figs. 6 and 7, respectively, for Langmuir and Freundlich adsorption isotherms. Both the equations were fitted in optimizing the two unknown parameters *viz*. q_m and K_a for Langmuir isotherm and K_F and $1/n$ for Freundlich adsorption isotherm. The data are reasonably fitted well to the Langmuir and Freundlich adsorption isotherms especially for the IIAC-Cu(II) systems as the least square sum was obtained in the range of 0.287–0.786. However, it was not well fitted to the IIAC-Pb(II) systems since the least square sum was found in the range of 0.669–7.756. Very high percent removal of lead(II) which was almost independent of concentration (ranging 1.0–20.0 ppm) was, perhaps, the reason of improper data fitting. Even the unknown parameters were estimated for both the ions and given in Table 1. The Langmuir constants q_m and K_a were found to be 2.887 mg/g and 0.363 (for IIAC-R-Cu(II)); 2.582 mg/g and 0.239 (for IIAC-N-Cu(II); 38.244 mg/g and 0.165 for (IIAC-R-Pb(II)); and 22.594 mg/g and 0.278 (for IIAC-N-Pb(II)), respectively. These results showed that very high removal capacity was obtained for the Pb(II) comparing to the Cu(II). The Cu(II) itself showed reasonably a high removal capacity. Moreover, these values showed significantly higher Langmuir monolayer capacity compared to the bare ACs as determined previously [46]. These results clearly showed that sorption capacity of these solids greatly enhanced when impregnated with iron. Further, it was reported that the q_m had influence on the heat of sorption: the higher the value of q_m, the stronger the bond formation that the heat of sorption forms [47]. The applicability of Langmuir adsorption isotherm pointed that the surface active sites were distributed evenly onto the surface. Similarly, it was also reported

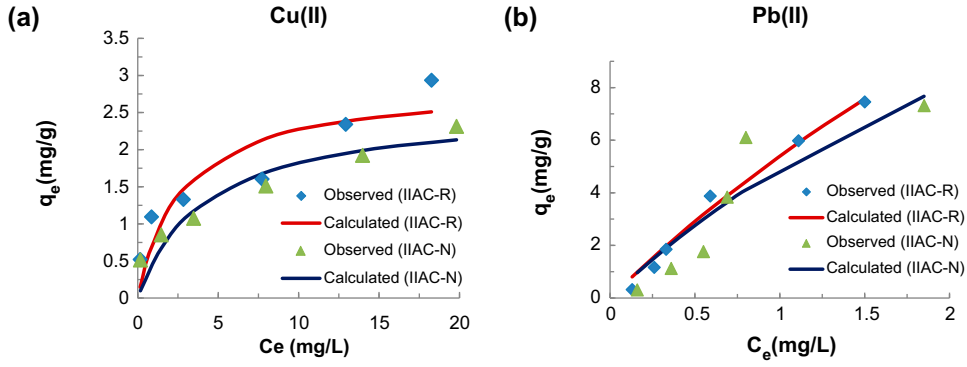

Fig. 6. Langmuir adsorption isotherms obtained for the adsorption of (a) Cu(II) and Pb(II) by using IIACs.

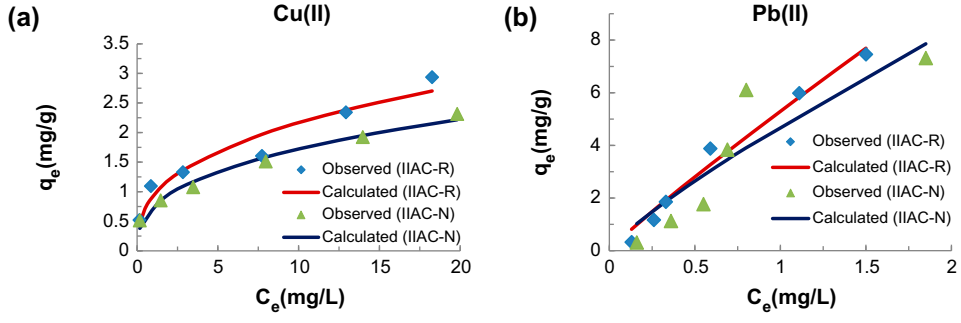

Fig. 7. Freundlich adsorption isotherms obtained for the adsorption of (a) Cu(II) and (b) Pb(II) by using IIACs.

Table 1
Langmuir and Freundlich adsorption isotherms data for the adsorption of Cu(II) and Pb(II) onto the solid surfaces

Materials	Langmuir Adsorption isotherm						Freundlich Adsorption isotherm					
	Cu(II)			Pb(II)			Cu(II)			Pb(II)		
	q_m	K_a	LSM	q_m	K_a	LSM	K_f	$1/n$	LSM	K_f	$1/n$	LSM
IIAC-R	2.887	0.363	0.786	38.244	0.165	0.670	0.927	0.368	0.242	5.296	0.920	0.838
IIAC-N	2.582	0.240	0.287	22.594	0.278	6.955	0.738	0.010	0.042	4.706	0.833	7.756
AC-R [45]	0.684	1.223	0.981*	5.348	0.155	0.928*	0.370	0.248	0.949*	0.727	0.704	0.983*
AC-N [45]	0.521	1.899	0.979*	5.000	0.140	0.969*	0.315	0.220	0.809*	0.636	0.699	0.991*

LSM: Least square sum.
*denotes: R^2.

previously that several biosorbents or chitosan-coated sand possessed higher Langmuir sorption capacity for Pb(II) than for Cu(II) even at different experimental conditions [48,49]. On the other hand, the Langmuir constant K_a was found to be related to the equilibrium constant of the sorption process of metal cations onto the solid surface [50] Eq. (7):

$$\mathrm{M(II)} + \mathrm{Solid} \leftrightarrow \mathrm{M(II)}\ldots\mathrm{Solid\ (Surface\ sorption\ complex)} \quad (7)$$

Reasonably, the low value obtained for these systems indicated the strong affinity and strength of the sorbent towards these two ions [21,31,51].

On the other hand, the Freundlich constants K_F and 1/n were computed: 0.927 mg/g and 0.368 for IIAC-R-Cu(II); 0.738 mg/g and 0.01 for IIAC-N-Cu(II); 5.296 mg/g and 0.920 for IIAC-R-Pb(II); 4.706 mg/g and 0.833 for IIAC-R-Pb(II), respectively. A marked difference in the sorption capacity estimated by the two different models for these two solids in the sorption of Cu(II) and Pb(II) was ascribed due to different basic assumptions. The applicability of the Freundlich adsorption isotherm indicated that the sorbing ions were aggregated by forming strong chemical bonds at the solid surface and likely to be interacted laterally; however, the Freundlich isotherm could not provide the information on the monolayer adsorption capacity [31,42,52,53]. Similar to the Langmuir isotherm, the sorption capacity is higher for Pb(II) than for Cu(II) using these two different solids. However, reasonably high sorption capacity was obtained for these two pollutants. Further, the 1/n values which relate to the adsorption intensity showed fractional values ($0 < 1/n < 1$), inferring a heterogeneous surface structure of solid surface with exponential distribution of active sites [52,54].

3.2.4. Adsorption dynamics

The sorption dynamics was carried out collecting the time dependence adsorption data for these two cations. The results obtained were presented graphically in Fig. 8(a) and (b), respectively, for Cu(II) and Pb(II) adsorption. Results clearly indicated that a very fast initial rise of adsorption was slowed down in the latter stage of contact time and it achieved

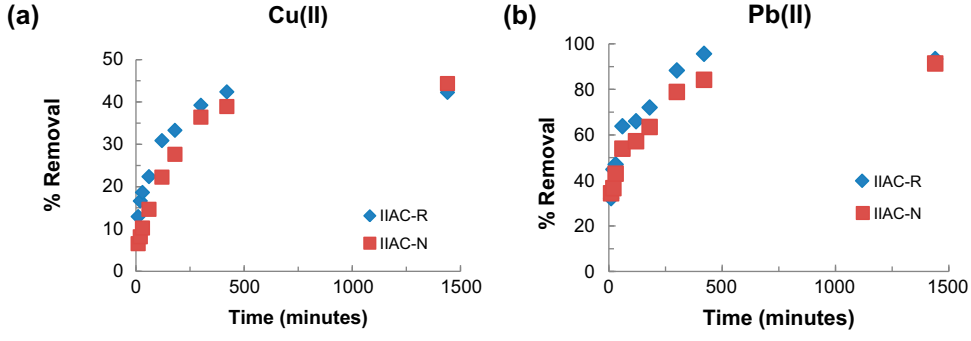

Fig. 8. Time dependence sorption of (a) Cu(II) and (b) Pb(II) by using IIACs.

almost a constant adsorption after about 400 min of contact. Moreover, the maximum adsorption was taken place within initial few minutes i.e. within 60–90 min of contact. Further, the time dependence data were utilized to discuss the kinetics of sorption using the pseudo-first-order and pseudo-second-order equations.

The Lagergren's pseudo-first-order kinetic model [53,55] was employed to its linear form (Eq. 8):

$$\log(q_e - q_t) = \log q_e - \frac{k_1}{2.303} \times t \quad (8)$$

where q_e and q_t (mg/g) are the amount of Cu(II) or Pb (II) adsorbed at equilibrium and at time t, respectively. The pseudo-first-order constant k_1 was obtained from the slope of the plot of Log (q_e–q_t) vs. t and results obtained were given in Table 2.

Similarly, the pseudo-second-order kinetic equation [56,57] was also employed to its linear form (Eq. 9):

$$\frac{t}{q_t} = \frac{1}{k_2 q_e^2} + \frac{t}{q_e} \quad (9)$$

where q_e is the maximum adsorption capacity (mg/g) and k_2 (g/mg/min) is the adsorption rate constant of pseudo-second order. From the plots of $\frac{t}{q_t}$ against t, the pseudo-second-order rate constant k_2 along with q_e was estimated for these two cations i.e. Cu(II) and Pb(II)) and given in Table 3. It was previously studied for the sorption of divalent metal cations onto the *sphagnum* moss peat and suggested that the uptake of metal cations followed the second-order rate laws. Further, it was suggested that the metals cations were bound onto the surface of biosorbent by the strong chemical forces which occurred between the valency forces sharing or the exchange of electrons and the peat and divalent metal ions forming covalent bonds; Eq. (9) was derived from its linear form [57,58]. It was, further, mentioned that the rate of second-order reaction could depend on the sorbate ion concentration available onto the surface and amount of sorbate ions sorbed at equilibrium [57,58].

It was observed that there was a reasonably good agreement between the kinetic data obtained for both pseudo-first-order and pseudo-second-order rate kinetics. Similarly, the sorption capacity of these solids for Cu(II) and Pb(II) was optimized, which again showed a very high removal capacity for these two cations. These results indicated that these solids have a reasonably fair affinity and potentiality towards the removal of Cu(II) and Pb(II). Between these two studied cations, the Pb(II) was removed at higher extent in comparison to Cu(II) using IIACs, which is in line with the previous observations obtained by the adsorption isotherm studies. Further, the applicability of pseudo-second-order kinetic model indicated again that "chemisorption" could be a predominant uptake

Table 2
Values of rate constants and maximum sorption capacities of IIACs obtained for the sorption of Cu(II) and Pb(II) using pseudo-first-order kinetic models

Materials	Pseudo-first-order					
	Cu(II)			Pb(II)		
	k_1 (1/min) × 10^{-3}	q_e (mg/g)	R^2	k_1 (1/min) × 10^{-3}	q_e (mg/g)	R^2
IIAC-R	7.37	1.189	0.993	6.68	2.321	0.949
IIAC-N	4.84	1.588	0.994	5.07	2.281	0.986

Table 3
Values of rate constants and maximum sorption capacities of IIACs obtained for the sorption of Cu(II) and Pb(II) using pseudo-second-order kinetic models

Materials	Pseudo-second-order					
	Cu(II)			Pb(II)		
	k_2 (g/mg/min)	q_e (mg/g)	R^2	k_2 (g/mg/min)	q_e (mg/g)	R^2
IIAC-R	12.22	1.770	0.990	10.05	3.507	0.983
IIAC-N	4.75	1.926	0.971	7.67	3.439	0.983

process for Cu(II) or Pb(II) sorption onto solid surfaces, which involved valency forces through sharing or exchanging electrons between the sorbent surface and the sorbate ions as also studied for different systems [58–61].

3.2.5. Effect of electrolyte concentrations

The electrolyte concentration is an important parameter which reveals the mechanism of sorption process; particularly, the nature of the binding of the sorbate ions onto the competing solid surfaces. The electrolyte concentration was increased from 0.001 to 1.0 mol/L $NaNO_3$ and the sorption of Cu(II) and Pb (II) was obtained by these solids. Results were presented in percent removal against an electrolyte concentration and given in Fig. 9(a) and (b) for Cu(II) and Pb(II), respectively. It was noted that increasing the electrolyte concentrations from 0.001 to 1.0 mol/L $NaNO_3$ (i.e. 1,000 times increase in the background electrolyte concentration) caused a decrease in the percent removal of Cu(II) by 12.51% and 13.96, respectively, for the solids IIAC-R and IIAC-N; and a decrease in the percent removal of Pb(II) by 10.09 and 1.60%, respectively, for the solids IIAC-R and IIAC-N. The insignificant decrease in the percent removal of Cu(II) or Pb(II) by these solids even with an increase in electrolyte concentrations for 1,000 times strongly favored that the Cu(II) or Pb(II) ions were adsorbed, predominantly, specifically onto the solid surface and form an "inner sphere complexes" onto the surface [62,63]. These results were in line with the kinetic studies which enabled the fair applicability of second-order-rate equation.

3.3. Fixed bed column studies

The fixed bed column studies were conducted, employing the column conditions as described previously. The breakthrough curves obtained for these systems were given in Fig. 10(a) and (b), respectively, for the Cu(II) and Pb(II). A close scrutiny of the figures revealed that a relatively high breakthrough volume was obtained for these two

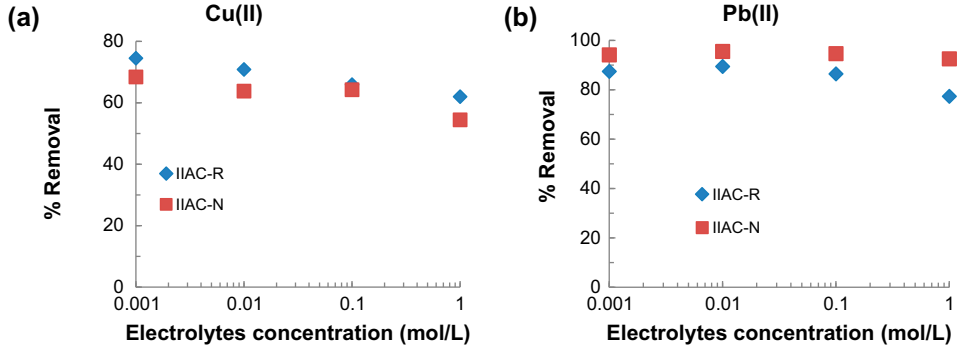

Fig. 9. Effect of electrolyte concentrations ($NaNO_3$) in the percent removal of (a) Cu(II) and (b) Pb(II) by using IIACs.

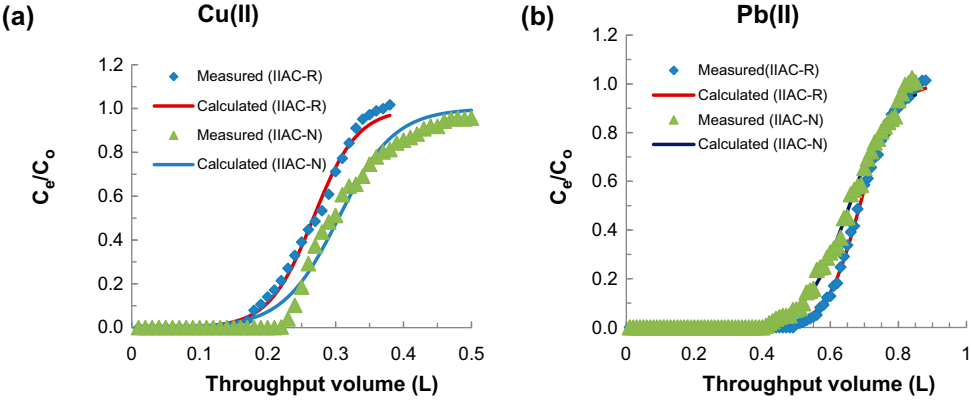

Fig. 10. Breakthrough curve obtained for the removal of (a) Cu(II) and (b) Pb(II) by IIACs.

Table 4
Thomas constants for the removal of Cu(II) and Pb(II) from aqueous solutions by different samples of IIACs

Materials	Cu(II)			Pb(II)		
	q_0 (mg/g)	K_T (L/min/mg) × 10^{-3}	Least square sum	q_0 (mg/g)	K_T (L/min/mg) × 10^{-3}	Least square sum
IIAC-R	2.746	2.97	2.9×10^{-2}	6.957	2.03	1.4×10^{-2}
IIAC-N	3.057	2.42	1.1×10^{-1}	6.505	1.58	3.5×10^{-2}
AC-R [45]	2.316	1.80	2.8×10^{-1}	5.960	1.92	1.8×10^{-1}
AC-N [45]	2.506	1.76	1.5×10^{-1}	4.932	2.26	3.3×10^{-2}

cations using these solid materials. Quantitatively, the complete breakthrough volume was obtained at 0.36, 0.54, 0.86, and 0.82 L for the systems IIAC-R-Cu(II), IIAC-N-Cu(II), IIAC-R-Pb(II), and IIAC-N-Pb(II), respectively. The high breakthrough volume obtained for these two cations indicated the strong affinity of these solids towards the metal cations, even under the dynamic conditions as well [64,65]. Moreover, it was pointed that a fixed bed process could have an additional advantage of a continuous contact between sorbate ions and solid surface, which may result in better exhaustion capacity than batch process [58,66].

Further, the breakthrough data were implied to obtain the loading capacity of these solids under the dynamic conditions using Thomas Eq. (10) to its non-linear form [67]:

$$\frac{C_e}{C_0} = \frac{1}{1 + e^{(K_T(q_0 m - C_0 V))/Q}} \tag{10}$$

where C_e and C_0 is the Cu(II)/Pb(II) concentration (mg/L) of effluent and influent solutions, respectively; K_T is Thomas rate constant (L/min/mg); q_0 is the maximum amount of Cu(II)/or Pb(II) that could be loaded (mg/g) in the column under the specified column conditions; m is the mass of adsorbent packed in column (g); V is the throughput volume (L); and Q is the flow rate of pumped Cu(II)/or Pb(II) solution (L/min). The pH of the influent solution was kept constant at 4.0. A non-linear least square fitting was conducted using the breakthrough column data. The fitting was performed with two unknown parameters, i.e. K_T and q_0 (*Cf* Fig. 10). The values of Thomas constants along with the least square sum obtained for these systems are given in Table 4. The data clearly indicated that a very high loading capacity was achieved for both Cu(II) and Pb(II) by these solids even under the dynamic conditions, which showed a better potential affinity of solids at least for these two cations. Comparatively, Pb(II) possessed higher loading capacity than Cu(II), which is in line with the previous batch data discussed before. These results were similar to the findings of batch reactor experiments and to other reports in which Thomas equation was fitted well to demonstrate the loading capacity of different sorbents [30,68]. The loading capacity for the AC samples was also included for its comparison, which clearly indicated that the iron impregnation enhanced the capacity of these two solids at least for the removal of Cu(II) and Pb(II) from aqueous solutions.

4. Conclusions

The agricultural by-products/wastes *viz*., rice hulls and *areca* nut waste were employed to obtain the ACs in an attempt to obtain cost-effective and environmentally benign materials. Further, the large specific surface area was utilized to impregnate it with lower dose of iron so as to obtain the IIACs. The solids were characterized with the IR and XRD analyses. Moreover, the surface morphology was obtained with SEM images. Results showed that iron was clustered/impregnated onto the surface and within the pores of the ACs. The BET specific surface area was slightly, but significantly, decreased in the presence of iron. The batch reactor data obtained for various physicochemical parametric studies showed that an increase in the pH greatly favored the removal of Cu(II) and Pb(II); whereas, an increase in the sorbate concentration showed a marked decrease in the percent removal of Cu(II) whereas Pb(II) was almost unaffected for such sorbate concentration increase. The equilibrium state sorption data were reasonably fitted well to the Langmuir and Freundlich adsorption isotherms and, hence, the removal capacity was estimated. The kinetic data showed that a fast initial removal was occurred for both Cu(II) and Pb(II) by these solids and the maximum sorption took place between 60 and 90 min of contact. The data are fitted well to the pseudo-first-order and pseudo-second-order rate equations. The sorption capacity estimated by the pseudo-second-order

equation fitting was found to be 1.770, 1.926, 3.507, and 3.439 mg/g, respectively, for the systems IIAC-R-Cu(II), IIAC-N-Cu(II), IIAC-R-Pb(II), and IIAC-N-Pb (II). The uptake of these ions onto the employed solids was almost unaffected by an increase in 1,000 times electrolyte concentration ($NaNO_3$), which showed that sorbing ions were forming a strong bond at the surface functional groups and, perhaps, making an "inner-sphere complexes." The column reactor operations revealed that relatively high breakthrough volume was obtained for the Cu(II) and Pb(II) and the breakthrough data were reasonably fitted well to Thomas equation. Therefore, the loading capacities were estimated for these two materials. The obtained loading capacity was higher for Pb(II) than for Cu(II) by IIACs. Moreover, both the IIACs, i.e. IIAC-R and IIAC-N, showed a comparable removal behavior at least for Cu(II) and Pb(II). Further, it was revealed that the impregnation of ACs samples with iron significantly enhanced the removal capacities of ACs samples at least for the removal of Cu(II) and Pb(II) from aqueous solutions. This study includes a comprehensive data which could further be employed in the remediation of copper- or lead-contaminated aquatic environment using IIACs materials at pilot plant scale or large-scale.

Acknowledgement

This work was supported by the National Research Foundation of Korea (NRF) grant funded by the Korea government (MEST) (No. 2012R1A2A4A01001539).

References

[1] V.M. Gun'ko, R. Leboda, J. Skubiszewska-Zie ba, P. Oleszczuk, Carbon adsorbents from waste ion-exchange resins, Carbon 43 (2005) 1143–1150.
[2] M. Ahmedna, W.E. Marshall, A.A. Husseiny, R.M. Rao, I. Goktepe, The use of nutshell carbons in drinking water filters for removal of trace metals, Water Res. 38 (2004) 1062–1068.
[3] M. Pesvento, A. Profumo, G. Alberti, F. Conti, Adsorption of lead(II) and copper(II) by complexation with surface functional groups, Anal. Chim. Acta 480 (2003) 171–180.
[4] J.W. Kim, M.H. Sohn, D.S. Kim, S.M. Sohn, Y.S. Kwon, Production of granular activated carbon from waste walnut shell and its adsorption characteristics for Cu2+ ion, J. Hazard. Mater. 85 (2001) 301–315.
[5] M.O. Corapcioglu, C.P. Huang, The adsorption of heavy metals onto activated carbon, Water Res. 21 (1987) 1031–1044.
[6] M. Imamoglu, O. Tekir, Removal of copper(II) and lead(II) ions from aqueous solutions by adsorption on activated carbon from a new precursor hazelnut husks, Desalination 228 (2008) 108–113.
[7] M. Kazemipour, M. Ansari, S. Tajrobehkar, M. Majdzadeh, H.R. Kermani, Removal of lead, cadmium, zinc, and copper from industrial wastewater by carbon developed from walnut, hazelnut, almond, pistachio shell, and apricot stone, J. Hazard. Mater. 150 (2008) 322–327.
[8] M. Teker, O. Saltabas, M. Imamoglu, Adsorption of cobalt by activated carbon from the rice hulls, J. Environ. Sci. Health., Part A Environ. Sci. Eng.Toxic Hazard. Subst. Control 32 (1997) 2077–2086.
[9] M. Ahmedna, W.F. Marshall, R.M. Rao, Production of granular activated carbons from select agricultural by-products and evaluation of their physical, chemical and adsorption properties, Bioresour. Technol. 71 (2000) 113–123.
[10] C. Sentorun-Shalaby, M.G. Ucak-Astarlioglu, L. Artok, C. Sarici, Preparation and characterization of activated carbons by one-step steam pyrolysis/activation from apricot stones, Microporous Mesoporous Mater. 88 (2006) 126–134.
[11] R. Malik, D.S. Ramkete, S.R. Wade, Adsorption of malachite green on groundnut shell waste based powdered activated carbon, J. Waste Manage. 27 (2007) 1129–1138.
[12] K. Kadirvelu, M. Kavipriya, C. Karthika, M. Radhika, N. Vennilamani, S. Pattabhi, Utilization of various agricultural wastes for activated carbon preparation and application for the removal of dyes and metal ions from aqueous solutions, Bioresour. Technol. 87 (2003) 129–132.
[13] V.K. Gupta, I. Ali, V.K. Saini, Defluoridation of wastewaters using waste carbon slurry, Water Res. 41 (2007) 3307–3316.
[14] V.K. Gupta, B. Gupta, A. Rastogi, S. Agarwal, A. Nayak, A comparative investigation on adsorption performance of mesoporous activated carbon prepared from waste rubber tire and activated carbon for a hazardous azo dye-Acid Blue 113, J. Hazard. Mater. 186 (2011) 891–901.
[15] G. Moussavi, A. Alahabadi, K. Yaghmaeian, M. Eskandari, Preparation, characterization and adsorption potential of the NH4Cl-induced activated carbon for the removal of amoxicillin antibiotic from water, Chem. Eng. J. 217 (2013) 119–128.
[16] R.S. Ribeiro, N.A. Fathy, A.A. Attia, A.M.T. Silva, J.L. Faria, H.T. Gomes, Activated carbon xerogels for the removal of the anionic azo dyes Orange II and Chromotrope 2R by adsorption and catalytic wet peroxide oxidation, Chem. Eng. J. 195–196 (2012) 112–121.
[17] D. Tiwari, S.M. Lee, Biomass-derived materials in the remediation of heavy-metal contaminated water: Removal of cadmium(II) and copper(II) from aqueous solutions, Water Environ. Res. 83 (2011) 874–881.
[18] A.K. Jain, V.K. Gupta, A. Bhatnagar, Suhas, A comparative study of adsorbents prepared from industrial wastes for removal of dyes, Sep. Sci. Technol. 38 (2003) 463–481.
[19] V.K. Gupta, S. Sharma, Removal of zinc from aqueous solutions using Bagasse fly ash—A low cost adsorbent, Ind. Eng. Chem. Res. 42 (2003) 6619–6624.
[20] A.H. Sulaymon, B.A. Abid, J.A. Al-Najar, Removal of lead copper chromium and cobalt ions onto granular

activated carbon in batch and fixed-bed adsorbers, Chem. Eng. J. 155 (2009) 647–653.
[21] Lalhmunsiama, D. Tiwari, S.M. Lee, Activated carbon and manganese coated activated carbon precursor to dead biomass in the remediation of arsenic contaminated water, Environ. Eng. Res. 17(S1) (2012) S41–S48.
[22] W. Liu, J. Zhang, C. Zhang, Y. Wang, Y. Li, Adsorptive removal of Cr(VI) by Fe-modified activated carbon prepared from Trapa natans husk, Chem. Eng. J. 162 (2010) 677–684.
[23] Z.M. Gu, J. Fang, B.L. Deng, Preparation and evaluation of GAC-based iron containing adsorbents for arsenic removal, Environ. Sci. Technol. 39 (2005) 3833–3843.
[24] V. Fierro, G. Muniz, G. Gonzalez-Sanchezc, M.L. Ballinsab, A. Celzarda, Arsenic removal by iron-doped activated carbons prepared by ferric chloride forced hydrolysis, J. Hazard. Mater. 168 (2009) 430–437.
[25] T. Depci, Comparison of activated carbon and iron impregnated activated carbon derived from Golbasi lignite to remove cyanide from water, Chem. Eng. J. 181–182 (2012) 467–478.
[26] V.K. Gupta, S. Agarwal, T.A. Saleh, Chromium removal by combining the magnetic properties of iron oxide with adsorption properties of carbon nanotubes, Water Res. 45 (2011) 2207–2212.
[27] T.A. Saleh, V.K. Gupta, Column with CNT/mangnisiumoxide composite for lead(II) removal from water, Environ. Sci. Pollut. Res. 19 (2012) 1224–1228.
[28] S. Hydari, H. Sharififard, M. Nabavinia, M.R. Parvizi, A comparative investigation on removal performances of commercial activated carbon, chitosan biosorbent and chitosan/activated carbon composite for cadmium, Chem. Eng. J. 193–194 (2012) 276–282.
[29] M. Irani, A.R. Keshtkar, M.A. Moosaviaan, Removal of cadmium from aqueous solution using mesoporous PVA/TEOS/APTES composite nanofiber prepared by sol-gel/electrospinning, Chem. Eng. J. 200–202 (2012) 192–201.
[30] D. Tiwari, S.M. Lee, Novel hybrid materials in the remediation of ground waters contaminated with As (III) and As(V), Chem. Eng. J. 204–206 (2012) 23–31.
[31] D. Tiwari, H.U. Kim, S.M. Lee, Removal behavior of sericite for Cu(II) and Pb(II) from aqueous solutions: Batch and column studies, Sep. Purif. Technol. 57 (2007) 11–16.
[32] V. Gomez-Serrano, J. Pastor-Villegas, A. Perez-Florindo, C. Duran-Valle, C. Valenzuela-Calahorro, FT-IR study of rockrose and of char and activated carbon, J. Anal. Appl. Pyrolysis 36 (1996) 71–80.
[33] A.M. Puziy, O.I. Poddubnaya, A. Martinez-Alonso, F. Suarez-Garcia, J.M.D. Tascon, Synthetic carbons activated with phosphoric acid I: Surface chemistry and ion binding properties, Carbon 40 (2002) 1493–1505.
[34] M. Al Bahri, L. Calvo, M.A. Gilarranz, J.J. Rodriguez, Activated carbon from grape seeds upon chemical activation with phosphoric acid: Application to the adsorption of diuron from water, Chem. Eng. J. 203 (2012) 348–356.
[35] J. Kong, Q. Yue, L. Huang, Y. Gao, Y. Sun, B. Gao, Q. Li, Y. Wang, Preparation, characterization and evaluation of adsorptive properties of leather waste based activated carbon via physical and chemical activation, Chem. Eng. J. 221 (2013) 62–71.
[36] S.M. Rodulfo-Baechler, S.L. Gonalez-Cortes, J. Orozco, V. Sagredo, B. Fontal, A.J. Mora, G. Delgado, Characterization of modified iron catalysts by X-ray diffraction, infrared spectroscopy, magnetic susceptibility and thermo gravimetric analysis, Mater. Lett. 58 (2004) 2447–2450.
[37] Y.S. Li, J.S. Church, A.L. Woodhead, F. Moussa, Preparation and characterization of silica coated iron oxide magnetic nano-particles, Spectrochim. Acta, Part A 76 (2010) 484–489.
[38] Y. Liu, Y. Guo, W. Gao, Z. Wang, Y. Ma, Z. Wang, Simultaneous preparation of silica and activated carbon from rice husk ash, J. Cleaner Prod. 32 (2012) 204–209.
[39] A.V. Vitela-Rodriguez, J.R. Rangel-Mendez, Arsenic removal by modified activated carbons with iron hydro(oxide) nanoparticles, J. Environ. Manage. 114 (2013) 225–231.
[40] G. Muniz, V. Fierro, A. Celzard, G. Furdin, G. Gonzalez-Sanchez, M.L. Ballinas, Synthesis, characterization and performance in arsenic removal of iron-doped activated carbons prepared by impregnation with Fe(III) and Fe(II), J. Hazard. Mater. 165 (2009) 893–902.
[41] D. Tiwari, C. Laldanwngliana, C.H. Choi, S.M. Lee, Manganese-modified natural sand in the remediation of aquatic environment contaminated with heavy metal toxic ions, Chem. Eng. J. 171 (2011) 958–966.
[42] S.M. Lee, C. Laldawngliana, D. Tiwari, Iron-immobilized-sand material in the treatment of Cu(II), Cd(II) and Pb(II) contaminated waters, Chem. Eng. J. 195–196 (2012) 103–111.
[43] N. Tewari, P. Vasudevan, B.K. Guha, Study on biosorption of Cr(VI) by Mucor heimalis, Biochem. Eng. J. 23 (2005) 185–192.
[44] Z. Aksu, Determination of the equilibrium, kinetic and thermodynamic parameter of the batch biosorption of nickel(II) ions onto C. vulgaris, Process Biochem. 38 (2002) 89–99.
[45] M. Machida, M. Aikawa, H. Tatsumoto, Prediction of simultaneous adsorption of Cu(II) and Pb(II) onto activated carbon by conventional Langmuir type equations, Hazard. Mater. 120 (2005) 271.
[46] Lalhmunsiama, S.M. Lee, D. Tiwari, Manganese oxide immobilized activated carbons in the remediation of aqueous wastes contaminated with copper(II) and lead(II), Chem. Eng. J. 225 (2013) 128–137.
[47] A.E. Ofomaja, E.I. Unuabonah, N.A. Oladoja, Competitive modeling for the biosorptive removal of copper and lead ions from aqueous solution by Mansonia wood sawdust, Bioresour. Technol. 101 (2010) 3844–3852.
[48] M.W. Wan, C.C. Kan, B.D. Rogel, M.L.P. Dalida, Adsorption of copper(II) and lead(II) ions from aqueous solution on chitosan-coated sand, Carbohydr. Polym. 80 (2010) 891–899.
[49] S.Y. Quek, B. Al-Duri, D.A.J. Wase, C.F. Forster, Coir as a biosorbent of copper and lead, Trans I. Chem. E 76 (1998) 50–54.
[50] V.K. Gupta, V.K. Saini, N. Jain, Adsorption of As(III) from aqueous solutions by iron-coated sand, J. Colloid Interface Sci. 288 (2005) 55–60.

[51] A. Mittal, L. Kurup (Krishnan), V.K. Gupta, Use of waste materials-bottom ash and de-oiled soya, as potential adsorbents for the removal of Amaranth from aqueous solutions, J. Hazard. Mater. B117 (2005) 171–178.
[52] W.B. Lu, J.J. Shi, C.H. Wang, J.S. Chang, Biosorption of lead, copper and cadmium by an indigenous isolate Enterobacter sp. J1 possessing high heavy-metal resistance, J. Hazard. Mater. B134 (2006) 80–86.
[53] D.G. Cetinkaya, Z. Aksu, A. Ozturk, T. Kutsal, A comparative study on heavy-metal biosorption characteristics of some algae, Process Biochem. 34 (1999) 885–892.
[54] P. Benes, V. Majer, Trace Chemistry of Aqueous solutions. Elsevier, Amsterdam, 1980.
[55] S. Lagergren, Zur theorie der sogenannten adsorption geloster stoffe [The theory of adsorption for dissolved substances], K. Sven. Vetenskapsakad, Handl 24 (1898) 1–39.
[56] Y.S. Ho, Adsorption of heavy metals from waste streams by peat, Ph.D. Thesis, University of Birmingham, Birmingham, 1995.
[57] Y.S. Ho, Review of second-order model for adsorption systems, J. Hazard. Mater. B136 (2006) 681–689.
[58] Y.S. Ho, G. McKay, The kinetics of sorption of divalent metal ions onto sphagnum moss peat, Water Res. 34 (2000) 735–742.
[59] A. Mittal, D. Kaur, A. Malviya, J. Mittal, V.K. Gupta, Adsorption studies on the removal of coloring agent phenol red from wastewater using waste materials as adsorbents, J. Colloid Interface Sci. 337 (2009) 345–354.
[60] S. Sivrikaya, S. Albayrak, M. Imamoglu, A. Gundogdu, C. Duran, H. Yildiz, Dehydrated hazelnut husk carbon: a novel sorbent for removal of Ni(II) ions from aqueous solution, Desalin. Water Treat. 50 (2012) 2–13.
[61] C. Ozer, M. Imamoglu, Y. Turhan, F. Boysan, Removal of methylene blue from aqueous solutions using phosphoric acid activated carbon produced from hazelnut husks, Toxicol. Environ. Chem. 94 (2012) 1283–1293.
[62] K.B. Payne, T.M. Abdel-Fattah, Adsorption of arsenate and arsenite by iron-treated activated carbon and zeolites: Effects of pH, temperature and ionic strength, J. Environ. Sci. Health 40 (2005) 723–774.
[63] T.D. Schmidt, N. Vlasova, D. Zuzaan, M. Kersten, B. Daus, Adsorption mechanism of arsenate by zirconyl-functionalized activated carbon, J. Colloid Interface Sci. 317 (2008) 228–234.
[64] J.T. Matheickal, Q. Yu, Biosorption of lead(II) and copper(II) from aqueous solutions by pre-treated biomass of Australian marine algae, Bioresour. Technol. 69 (1999) 223–229.
[65] M.A. Stylianou, M.P. Hadjiconstantinou, V.J. Inglezakis, K.G. Moustakas, M.D. Loizidou, Use of natural clinoptilolite for the removal of lead, copper and zinc in fixed bed column, J. Hazard. Mater. 143 (2007) 575–581.
[66] A. Adak, M. Bandyopadhyay, A. Pal, Fixed bed column study for the removal of crystal violet (C.I. Basic Violet 3) dye from aquatic environment by surfactant-modified alumina, Dyes Pigm. 69 (2006) 245–251.
[67] H.C. Thomas, Heterogeneous ion exchange in a flowing system, J. Am. Chem. Soc. 66 (1944) 1664–1666.
[68] A. Singh, D. Kumar, J.P. Gaur, Continuous metal removal from solution and industrial effluents using Spirogyra biomass-packed column reactor, Water Res. 46 (2012) 779–788.